https://doi.org/10.21320/1818-474X-2024-2-62-72

The role of electrical impedance tomography in predicting the failure of non-invasive ventilation in patients with COVID-19-associated hypoxemic acute respiratory failure: a prospective observational study

A.P. Krasnoshchekova, A.I. Yaroshetskiy*, T.S. Serkova, Z.M. Merzhoeva, N.V. Trushenko, G.S. Nuralieva, N.A. Tsareva, S.N. Avdeev

Sechenov First Moscow State Medical University (Sechenov University), Moscow, Russia

Роль электроимпедансной томографии в прогнозировании неудач неинвазивной вентиляции легких у пациентов с COVID-19-ассоциированной гипоксемической острой дыхательной недостаточностью: проспективное наблюдательное исследование

А.П. Краснощекова, А.И. Ярошецкий*, Т.С. Серкова, З.М. Мержоева, Н.В. Трушенко, Г.С. Нуралиева, Н.А. Царева, С.Н. Авдеев

ФГАОУ ВО «Первый Московский государственный медицинский университет им. И.М. Сеченова» Минздрава России (Сеченовский Университет), Москва, Россия

Abstract

INTRODUCTION: Data on prediction of the failure of non-invasive lung ventilation (NIV) in patients with respiratory failure associated with COVID-19, based on electrical impedance tomography (EIT) patterns are limited. **OBJECTIVE:** To identify predictors of non-invasive lung ventilation failure in patients with respiratory insufficiency associated with COVID-19, using electrical impedance tomography data. **MATERIALS AND METHODS:** A monocenter prospective cohort observational study was conducted in patients with moderate-to-severe COVID-19-associated acute respiratory failure, who underwent NIV in the ICU ($n = 43$). EIT was used to measure the actual ventilation area (S_{VENT}), hyperinflation area (S_{HYPER}), ventilation delay zone (S_{RVD}), and calculate the proportion of ventilated lungs (A_{VENT}), proportion of hyperinflation area (Z_{HYPER}), proportion of RVD area (Z_{RVD}), as well as the duration of hyperinflation during one respiratory cycle (T_{HYPER}), and the ratio of hyperinflation time to inhalation time. **RESULTS:** The study included 43 patients admitted 15 (10–22) days after the onset of COVID-19. Patients with NIV failure ($n = 34$) had higher Z_{HYPER} values on the first day (19.5 (16.3–30.5) in the NIV success group and 35.2 (25.0–45.0) in the failure group, AUROC 0.80, $p = 0.004$, Cut-off 39.7, Se 85 %, Sp 89 %) and the last day (20.6 (10.4–28.5) in the success group and 32.7 (26.4–43.3) in the failure group, AUROC 0.92, $p = 0.003$, Cut-off 32.7, Se 50 %, Sp 100 %), as well as a higher T_{HYPER}/T_{INSP} ratio on the last day of NIV (37.5

Реферат

АКТУАЛЬНОСТЬ: Данные о прогнозировании неудач неинвазивной вентиляции легких (НИВЛ) у пациентов с прогрессированием дыхательной недостаточности, ассоциированной с COVID-19, на основании изменения картины электроимпедансной томографии (ЭИТ) в динамике ограничены. **ЦЕЛЬ ИССЛЕДОВАНИЯ:** Поиск предикторов неудачи НИВЛ у пациентов с прогрессированием дыхательной недостаточности, ассоциированной с COVID-19, на основании данных ЭИТ. **МАТЕРИАЛЫ И МЕТОДЫ:** Моноцентровое проспективное когортное обсервационное исследование пациентов с COVID-19-ассоциированной острой дыхательной недостаточностью средней и тяжелой степени, которым применяли НИВЛ в отделениях реанимации и интенсивной терапии ($n = 43$). С помощью ЭИТ измеряли площадь фактической вентиляции (S_{VENT}), область гиперинфляции (S_{HYPER}), зону задержек вентиляции (S_{RVD}) и рассчитывали долю вентилируемых легких (A_{VENT}), долю зоны гиперинфляции (Z_{HYPER}), долю зоны RVD (Z_{RVD}), а также продолжительность гиперинфляции за время одного дыхательного цикла (T_{HYPER}) и отношение времени гиперинфляции ко времени вдоха. **РЕЗУЛЬТАТЫ:** В исследование включены пациенты ($n = 43$) на 15-е (10–22) сутки от начала заболевания. Пациенты с неудачей НИВЛ ($n = 34$) имели более высокие показатели Z_{HYPER} в первый день (19,5 (16,3–30,5) в группе успеха и 35,2 (25,0–45,0) в группе неудачи; AUROC 0,80,

(31.0–47.9) in the success group and 65.3 (43.7–88.4) in the failure group, AUROC 0.87, $p = 0.001$, Cut-off 52.7, Se 71 %, Sp 100 %). A_{VENT}, Z_{RVD}, and inhalation time did not show prognostic significance. **CONCLUSIONS:** EIT can predict the NIV failure in moderate-to-severe ARDS associated with COVID-19, based on the assessment of alveolar overdistention zones. Further research are needed to investigate this theory.

KEYWORDS: electrical impedance tomography, noninvasive ventilation, COVID-19, SARS-CoV-2, pneumonia, hospital mortality, respiratory support

* *For correspondence:* Andrey I. Yaroshetskiy — Dr. Med. Sci., PhD, ScD, professor, Pulmonology Department, Sechenov First Moscow State Medical University, Moscow, Russia;
e-mail: yaroshetskiy_a_i@staff.sechenov.ru

For citation: Krasnoshchekova A.P., Yaroshetskiy A.I., Serkova T.S., Merzhoeva Z.M., Trushenko N.V., Nuralieva G.S., Tsareva N.A., Avdeev S.N. The role of electrical impedance tomography in predicting the failure of non-invasive ventilation in patients with COVID-19-associated hypoxemic acute respiratory failure: a prospective observational study. Annals of Critical Care. 2024;2:62–72.
https://doi.org/10.21320/1818-474X-2024-2-62-72

Received: 28.08.2023
Accepted: 28.02.2024
Published online: 27.04.2024

$p = 0{,}004$, Cut-off 39,7, Se 85 %, Sp 89 %) и в последний день (20,6 (10,4–28,5) в группе успеха и 32,7 (26,4–43,3) в группе неудачи; AUROC 0,92, $p = 0{,}003$, Cut-off 32,7, Se 50 %, Sp 100 %) и T_{HYPER}/T_{INSP} в последний день НИВЛ (37,5 (31,0–47,9) в группе успеха и 65,3 (43,7–88,4) в группе неудачи; AUROC 0,87, $p = 0{,}001$, Cut-off 52,7, Se 71 %, Sp 100 %). A_{VENT}, Z_{RVD} и время вдоха не показали своей прогностической значимости. **ВЫВОДЫ:** ЭИТ может прогнозировать неудачу НИВЛ при среднетяжелом и тяжелом остром респираторном дистресс-синдроме, связанном с COVID-19, на основании оценки зон перераздувания альвеол. Требуются дальнейшие исследования для изучения этой теории.

КЛЮЧЕВЫЕ СЛОВА: электроимпедансная томография, неинвазивная вентиляция легких, COVID-19, SARS-CoV-2-ассоциированная пневмония, летальность, респираторная поддержка

* *Для корреспонденции:* Ярошецкий Андрей Игоревич — д-р мед. наук, профессор кафедры пульмонологии, врач — анестезиолог-реаниматолог, ФГАОУ ВО «Первый МГМУ им. И.М. Сеченова» (Сеченовский Университет) Минздрава России, Москва, Россия;
e-mail: yaroshetskiy_a_i@staff.sechenov.ru

Для цитирования: Краснощекова А.П., Ярошецкий А.И., Серкова Т.С., Мержоева З.М., Трушенко Н.В., Нуралиева Г.С., Царева Н.А., Авдеев С.Н. Роль электроимпедансной томографии в прогнозировании неудач неинвазивной вентиляции легких у пациентов с COVID-19-ассоциированной гипоксемической острой дыхательной недостаточностью: проспективное наблюдательное исследование. Вестник интенсивной терапии им. А.И. Салтанова. 2024;2:62–72.
https://doi.org/10.21320/1818-474X-2024-2-62-72

Поступила: 28.08.2023
Принята к печати: 28.02.2024
Дата онлайн-публикации: 27.04.2024

DOI: 10.21320/1818-474X-2024-2-62-72

Introduction

Non-invasive ventilation (NIV) has become one of the main methods of respiratory support for hypoxemic acute respiratory failure (ARF) associated with COVID-19. The main characteristic of COVID-19-associated ARF is relatively low recruitability of the alveoli and predominantly mono organ (pulmonary) dysfunction [1–3]. That is why NIV has become one of the main methods of respiratory support for ARF associated with COVID-19 and has shown an advantage over invasive ventilation. However, prolongation of NIV in the presence of indications for tracheal intubation may have a negative impact on the outcome [4]. Therefore, early prediction of NIV failure is an important and still unsolved problem [5].

Electrical Impedance Tomography (EIT) is a non-invasive imaging technique that uses the measurement of tissue electrical conductivity to provide a non-invasive way to monitor changes in lung volumes and ventilation distribution. During inspiration, lung volumes increase and lead to

an increase in intrathoracic impedance, while during expiration, the impedance decreases [6]. EIT is capable of producing images that are comparable to those from computed tomography (CT), and can even replace it in situations where transporting a patient to the CT room is challenging [7–8]. EIT has several benefits, including continuous monitoring, ease of use, and the ability to detect uneven distribution of gas during ventilation, which is critical in assessing lung damage. These benefits make it especially useful for bedside adjustments of respiratory support parameters [9]. However, no study has yet been conducted to evaluate the prognostic effectiveness of EIT in patients with COVID-19 during non-invasive ventilation (NIV).

Therefore, this study was conducted to address the lack of studies assessing the effectiveness of EIT in predicting NIV failure in COVID-19 patients.

Objective

The study aimed to find predictors of NIV failure based on the analysis of electrical impedance tomography data in patients with hypoxemic ARF associated with COVID-19.

Materials and methods

A single-center prospective cohort observational study was conducted in the intensive care unit (ICU) of Clinical Hospital No. 4 of Sechenov University from January 25, 2021 to May 31, 2021. The study was approved by the Local Ethics Committee of Sechenov University (Protocol No. 20-20 of 15.07.2020). The study included ICU patients with confirmed COVID-19 and moderate-to-severe acute respiratory distress syndrome (ARDS) (according to the Berlin criteria). We included patients during the first Day of NIV. Switch of respiratory support to NIV occurred after failure of standard oxygen therapy (flow > 15 L/min) or CPAP therapy combined with low-flow oxygen therapy outside the ICU. Failure of low-flow oxygen and CPAP therapy was considered to be at least one of the following criteria: patient fatigue, accessory respiratory muscle scale score (according to Patrick W.C. et al.) 4–5 points [10], SpO_2 < 92 % with oxygen flow 15 l/min, respiratory rate (RR) more than 30 per minute. Pregnant women, patients less than 18 years or more than 80 years (due to the high frailty of patients over 80 years), patients with life-threatening cardiac arrhythmias and/or systolic blood pressure < 80 mmHg despite vasopressor support with norepinephrine at a dose of > 2 μg/kg/min were excluded from the study. We excluded patients with the presence of primary lung diseases (for example, interstitial lung diseases, pulmonary emphysema) or tumor metastases to the lungs, chronic decompensated extrapulmonary diseases with severe organ dysfunction (progression of cancer, liver cirrhosis, chronic heart failure), patients with Glasgow Coma Score less than 14 points, and swallowing disorders. All patients underwent NIV in the Pressure Support Ventilation mode through an oronasal mask using Trilogy 202 (Philips Respironics, USA), Savina Select E (Drager, Germany,) and Carestation 860 (GE, USA) devices with the following settings: CPAP 8–10 mbar, Pressure Support 4–10 mbar above CPAP and FiO_2 level sufficient to achieve SpO_2 93–95 %. We used intubation criteria by the current version of the "Temporary Guidelines for Prophylaxis, Diagnostic and Treatment of COVID-19 of the Ministry of Health of the Russian Federation" at the time of the study [11]: hypoxemia (SpO_2 < 92 %) despite high-flow oxygen therapy or NIV with FiO_2 100 % in the prone position; patient fatigue during high-flow oxygen therapy through nasal cannulas or NIV in the prone position with FiO_2 100 %; increase in visible chest excursion and/or involvement of accessory respiratory muscles despite high-flow oxygen therapy or NIV in the prone position with FiO_2 100 %; depression of consciousness or agitation; respiratory arrest; unstable hemodynamics.

All patients underwent EIT using a PulmoVista 500 device (Drager, Germany) with the belt placed in the fifth intercostal space on Days 1, 3, 5, 7, 10, and 14 from the start of NIV. EIT was performed in the supine position of the patient for 15 minutes. We saved the image received from the screen of the EIT device in the "Diagnostics" mode. Automatic scaling was used for processing because it automatically adjusts the color scale to represent the pixel with the maximum relative impedance change relative to the baseline taken at the end of expiration (black color), and colors these pixels white, and the areas of "non-maximal" impedance change colors shades of blue — the lighter the color, the greater the change in impedance. Thus, if there are zones with different colors at the end of inspiration, one can judge the heterogeneity of the distribution of ventilation in different zones of the lungs. In addition, in the "Diagnostics" mode of the EIT device, we assessed regional ventilation delays (RVD) and also recorded videos of several respiratory cycles to assess inspiratory time.

After acquiring the image in the "Diagnostics" mode, we measured some areas in the images (in pixels) at the end of inspiration using Adobe Photoshop CS software (Adobe, USA). Before starting all measurements, we estimated the expected area of "healthy" lungs (S_{LUNG}). To calculate it, we drew the patient's supposed healthy lung borders through the visible ventilated edges in the image as close as possible to the ribs. This was done to take into account non-ventilated areas associated with the thickness of the chest wall (because of obesity, for example). Next, we calculated the number of pixels of the actual ventilation area (S_{VENT}) (Figure 1, A, area inside the light gray line), as well as the hyperinflation area (S_{HYPER}) or the number of pixels in white zones (Figure 1, B, white area inside the red lines), measured the number of pixels in the yellow zone — the zone of ventilation delays (S_{RVD}) (Figure 1, C, yellow area inside the red line). After this, the proportion of ventilated lungs

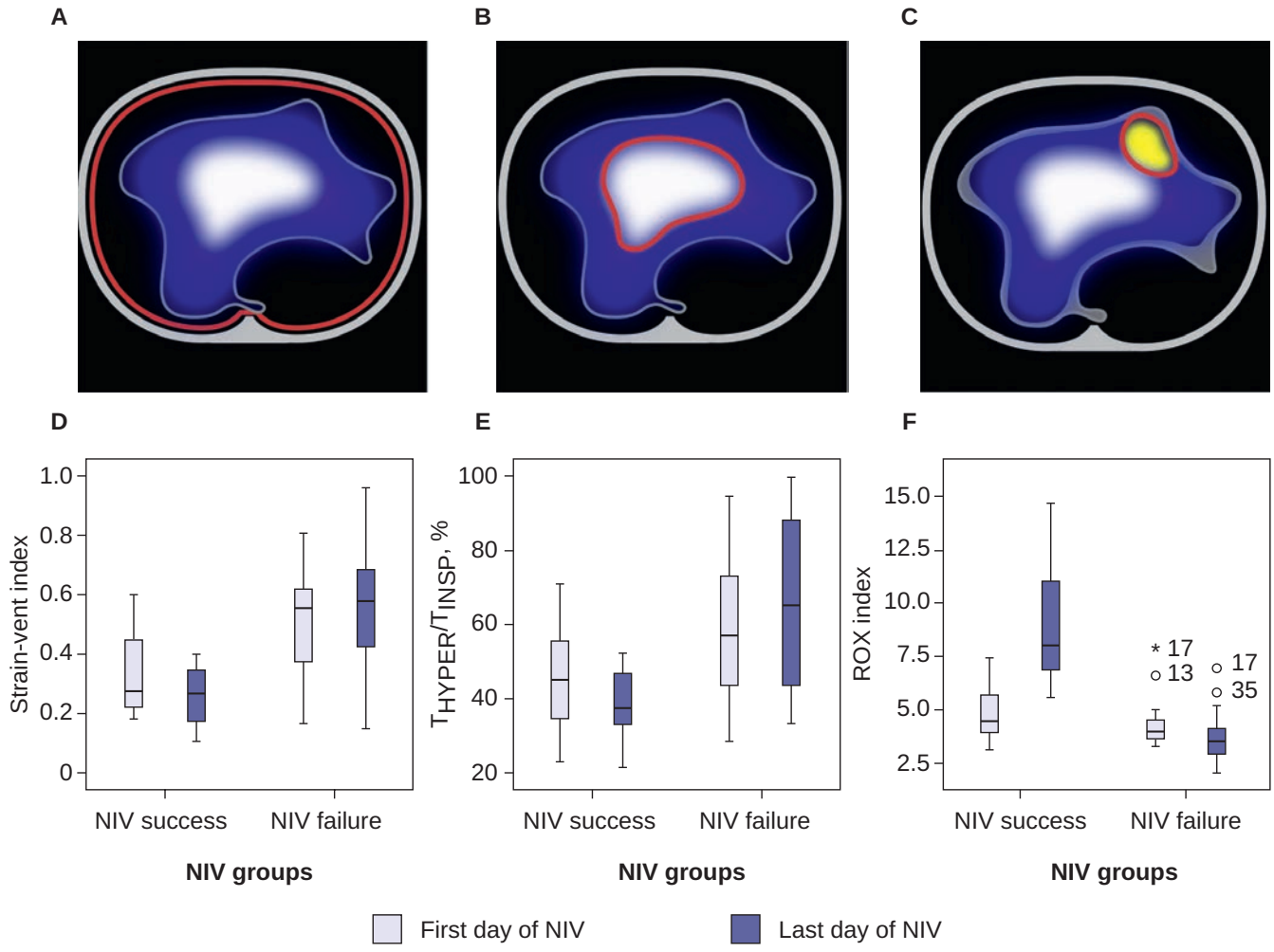

Fig. 1. *A–C*: Electrical impedance tomography image at the fifth intercostal space of a patient with COVID-19. Supposed lung area (S_{LUNG}) is the area inside the red line, drawn as a closed circle based on visible points of ventilation close to ribs; the area of ventilation S_{VENT} (blue zone) is the area inside the light grey line (*A*); the area of hyperinflation S_{HYPER} (white zone) is the white area inside the red line (*B*); regional ventilation delay (RVD) area S_{RVD} (yellow zone) is the yellow area inside the red line (*C*).

D–F: Electrical impedance tomography indexes and ROX index in non-invasive ventilation success and failure groups. Data presented as boxplots: grey depicts the 1st NIV day, and black — the last NIV day (within 24 hours before intubation in noninvasive ventilation failure group) (*D*); Strain-vent index; Time of hyperinflation to inspiratory time ratio (T_{HYPER}/T_{INSP}) (*E*); ROX index (*F*).

Note: The ROX index shows the ratio of arterial oxygen saturation (SpO_2) to the fraction of inspired oxygen (FiO_2), divided by the respiratory rate (RR): ROX = $SpO_2/FiO_2/RR$.

(A_{VENT}) was calculated as the ratio of the area of actual lungs to the area of "healthy" lungs S_{VENT}/S_{LUNG}. Hyperinflation zone share (Z_{HYPER}) — as the ratio of the area of bright white zones to the actual area of the lung S_{HYPER}/S_{VENT}. Also we calculated the share of the RVD zone (Z_{RVD}) as the ratio of the area of the yellow zones to the actual area of the lungs S_{RVD}/S_{VENT}.

Then we measured the duration of the white zones in the video during one breathing cycle (T_{HYPER}), assessing whether they appeared for a split second or took up the majority of the inspiration. After this, the ratio of the time of appearance of white zones in the video to the time of inspiration T_{HYPER}/T_{INSP} was calculated. We defined the "strain-vent index" as the ratio of the area of hyperinflation to the area of "healthy lungs" Z_{HYPER}/A_{VENT}. Also, the maximum RVD time was recorded.

We further measured respiratory rate, tidal volume (VT), inspiratory time, SpO_2, and arterial blood gases, and calculated the ROX index and ventilation coefficient (VR).

Descriptive statistics included medians and 25–75 % percentiles. To assess differences between groups, we used the Mann-Whitney *U*-test for continuous variables and the exact Chi-square test with Fisher's exact test for categorical variables. We performed ROC analysis to predict NIV failure when there were significant differences between groups. The null hypothesis was rejected at two-sided $p < 0.05$. Statistical analyses were performed using SPSS Statistics version 27.0 (IBM, Armonk, NY, USA).

Results

The study included 43 consecutive patients (men, *n* = 24), with a mean age of 73 (62–80) years, body mass index (BMI) of 30.5 (28.3–33.2) kg/m², mean time from the onset of the disease is 15 (10–22) days. 33 % of patients in the success group and 35 % in the failure group received CPAP therapy before transfer to the ICU. Baseline characteristics of the patients are presented in Table 1.

In 34 included patients, NIV was failed and respiratory support was escalated to invasive mechanical ventilation. Considering age and BMI of the included patients, they did not receive ECMO. There were no statistically significant differences in the NIV success and fNIV ailure groups on the day of NIV initiation. The groups were comparable in age, gender, BMI and comorbidities. Also, on the first day of NIV there were no differences in RR, PaO_2/FiO_2 and ROX index.

The proportion of ventilated lungs (A_{VENT}) increased in the success group and decreased in the failure group, although it did not show its predictive value (Table 2).

Patients with NIV failure (*n* = 34) had a higher percentage of white zones (Z_{HYPER}) on day 1: 19.5 (16.3–30.5) in the success group and 35.2 (25.0–45.0) in failure group (AUROC 0.80, *p* = 0.004, cut-off point 39.7 sensitivity 85 %, specificity 89 %), and on the last day of NIV (before intubation or before transfer from ICU): 20.6 (10.4–28.5) in the success group and 32.7 (26.4–43.3) in the failure group (AUROC 0.92 *p* = 0.003, cut-off point 32.7 sensitivity 50 %, specificity 100 %) (see Table 2).

Table 1. Baseline characteristics in non-invasive ventilation (NIV) success and NIV failure groups

Parameter	NIV success (*n* = 9)	NIV failure (*n* = 34)	*p*
Age, years	60.0 (56.5–63.0)	75.5 (69.5–80.3)	0.004
Men, *n*	4	20	0.345
BMI, kg/m²	31.6 (28.5–34.6)	30.1 (28.2–32.1)	0.303
Time from disease onset to ICU admission, days	14.0 (9.5–15.0)	15.0 (10.8–22.3)	0.173
NIV duration, days	9 (4–16)	5 (2–8)	0.074
CPAP outside the ICU, *n* (%)	3 (33)	12 (35)	0.734
Diabetes mellitus, *n* (%)	3 (33)	12 (35)	0.877
Ischemic heart disease, *n* (%)	3 (33)	9 (26)	0.846
Arterial hypertension, *n* (%)	7 (78)	27 (79)	1.000
Congestive heart failure, *n* (%)	1 (11)	2 (6)	0.424
Atrial fibrillation, *n* (%)	1 (11)	4 (12)	0.937
History of oncology, *n* (%)	1 (11)	3 (9)	0.327
History of myocardial infarction, *n* (%)	1 (11)	2 (6)	0.426

BMI — body mass index; NIV — noninvasive ventilation; ICU — intensive care unit.

Table 2. Respiratory and electrical impedance tomography parameters in non-invasive ventilation (NIV) success and NIV failure groups

Parameter	NIV success (*n* = 9)	NIV failure (*n* = 34)	*p*	ROC analysis		
				AUROC (95 % CI)	Cut-off	*p*
PaO_2/FiO_2, mmHg, Day 1	138 (91–177)	95 (86–113)	0.083	—	—	—
PaO_2/FiO_2, mmHg, Day 3	147 (113–195)	75 (67–91)	< 0.0001	0.93 (0.84–1.00)	< 111 (Se 94 %, Sp 87 %	< 0.0001
PaO_2/FiO_2, mmHg, Day 5	105 (79–134)	75 (72–89)	0.076	—	—	—
PaO_2/FiO_2, mmHg, Day 7	123 (96–248)	78 (69–123)	0.054	—	—	—
PaO_2/FiO_2, mmHg, the last NIV day	200 (139–248)	73 (64–96)	< 0.0001	0.97 (0.93–1.00)	< 122 (Se 91 %, Sp 100 %)	< 0.0001
RR, min^{-1}, Day 1	26 (22–29)	27 (25–29)	0.329	—	—	—
RR, min^{-1}, Day 3	23 (17–28)	28 (24–32)	0.022	—	—	—

Continuation of the tabl. 2

Parameter	NIV success (*n* = 9)	NIV failure (*n* = 34)	*p*	ROC analysis		
				AUROC (95 % CI)	Cut-off	*p*
RR, min^{-1}, Day 5	25 (21–29)	29 (25–33)	0.096	—	—	—
RR, min^{-1}, Day 7	23 (19–29)	26 (25–30)	0.208	—	—	—
RR, min^{-1}, the last NIV day	24 (17–26)	29 (25–33)	0.009	—	—	—
ROX index, Day 1	4.47 (3.78–6.09)	4.00 (3.63–4.54)	0.143	—	—	—
ROX index, Day 3	5.53 (4.72–11.36)	3.69 (3.24–4.41)	< 0.0001	0.92 (0.84–1.00)	< 4.58 (Se 85 %, Sp 88 %)	< 0.0001
ROX index, Day 5	5.49 (4.58–7.77)	3.55 (2.99–4.28)	0.003	—	—	—
ROX index, Day 7	5.53 (5.13–6.49)	3.81 (3.36–6.03)	0.079	—	—	—
ROX index, the last NIV day	8.03 (6.46–12.02)	3.48 (2.95–4.11)	< 0.0001	0.98 (0.96–1.00)	< 5.39 (Se 94 %, Sp 100 %)	< 0.0001
VR, Day 1	2.19 (1.60–3.01)	2.19 (1.96–2.74)	0.881	—	—	—
VR, Day 3	1.84 (1.57–2.34)	2.15 (1.76–2.90)	0.278	—	—	—
VR, Day 5	2.10 (1.52–2.71)	2.33 (1.74–2.51)	0.825	—	—	—
VR, Day 7	2.15 (1.70–2.31)	1.85 (1.50–2.34)	0.865	—	—	—
VR, the last NIV day	1.93 (1.54–2.18)	2.35 (1.81–2.95)	0.042	—	—	—
A_{VENT}, %, Day 1	70.7 (62.6–75.2)	70.3 (59.6–75.1)	0.988	—	—	—
A_{VENT}, %, Day 3	70.6 (58.8–76.2)	69.0 (53.0–80.0)	0.948	—	—	—
A_{VENT}, %, Day 5	71.6 (54.0–76.3)	69.5 (53.8–75.4)	0.768	—	—	—
A_{VENT}, %, Day 7	71.8 (58.7–79.2)	69.0 (54.2–72.9)	0.533	—	—	—
A_{VENT}, %, the last NIV day	75.7 (71.4–78.0)	64.3 (53.2–71.4)	0.007	—	—	—
Z_{HYPER}, %, Day 1	19.5 (16.3–30.5)	35.2 (25.0–45.0)	0.004	0.80 (0.65–0.96)	39.7 (Se 85 %, Sp 89 %)	0.005
Z_{HYPER}, %, Day 3	21.8 (10.1–41.7)	34.6 (27.0–47.8)	0.058	—	—	—
Z_{HYPER}, %, Day 5	27.4 (19.7–37.0)	40.8 (24.0–50.8)	0.130	—	—	—
Z_{HYPER}, %, Day 7	26.0 (21.8–39.8)	35.0 (27.6–45.5)	0.125	—	—	—
Z_{HYPER}, %, the last NIV day	20.6 (10.4–28.5)	32.7 (26.4–43.3)	0.003	0.92 (0.84–1.00)	32.7 (Se 50 %, Sp 100 %)	< 0.0001
T_{HYPER}/T_{INSP}, %, Day 1	44.9 (29.9–57.8)	57.1 (43.5–73.5)	0.052	—	—	—
T_{HYPER}/T_{INSP}, %, Day 3	45.3 (28.5–48.3)	58.8 (46.7–86.6)	0.021	—	—	—
T_{HYPER}/T_{INSP}, %, Day 5	39.7 (28.7–72.1)	68.7 (63.6–83.3)	0.065	—	—	—
T_{HYPER}/T_{INSP}, %, Day 7	49.2 (35.7–61.4)	70.0 (53.3–96.3)	0.047	—	—	—
T_{HYPER}/T_{INSP}, %, the last NIV day	37.5 (31.0–47.9)	65.3 (43.7–88.4)	0.001	0.87 (0.76–0.98)	> 52.7 (Se 71 %, Sp 100 %)	0.001
Strain-vent-index, Day 1	27.6 (22.0–48.6)	55.6 (37.2–62.4)	0.005	0.81 (0.65–0.97)	> 45.0 (Se 65 %, Sp 78 %)	0.005
Strain-vent-index, Day 3	30.9 (16.3–61.3)	56.0 (39.7–71.7)	0.056	—	—	—
Strain-vent-index, Day 5	42.8 (25.3–60.1)	60.7 (42.9–83.4)	0.238	—	—	—
Strain-vent-index, Day 7	35.7 (27.8–69.2)	59.0 (46.8–73.9)	0.157	—	—	—
Strain-vent-index, the last NIV day	26.9 (16.4–37.2)	57.9 (42.4–68.8)	< 0.0001	0.92 (0.84–1.00)	> 39.7 (Se 85 %, Sp 89 %)	< 0.0001
Z_{RVD}, %, Day 1	1.2 (0.0–16.0)	5.0 (0.8–11.9)	0.566	—	—	—
Z_{RVD}, %, Day 3	7.4 (0.0–11.6)	5.0 (0.5–13.3)	0.855	—	—	—
Z_{RVD}, %, Day 5	4.5 (0.0–10.3)	5.8 (0.5–11.8)	0.709	—	—	—

End of the tabl. 2

Parameter	NIV success (*n* = 9)	NIV failure (*n* = 34)	*p*	ROC analysis		
				AUROC (95 % CI)	Cut-off	*p*
Z_{RVD}, %, Day 7	0.0 (0.0–14.0)	2.0 (0.0–12.0)	0.595	—	—	—
Z_{RVD}, %, the last NIV day	9.0 (0.0–13.0)	5.8 (0.8–13.7)	1.000	—	—	—

Data are presented as median (interquartile range), except for ROC analysis.
A_{VENT} — ratio of ventilation area to estimated lung area; PaO_2/FiO_2 — ratio of oxygen tension in arterial blood to the inspiratory oxygen fraction; ROC: Se — sensitivity; Sp — specificity; ROX index — ratio of arterial oxygen saturation to fraction of inspired oxygen divided by RR (ROX index = $SpO_2/FiO_2/RR$); RR — respiratory rate; Strain-vent-индексindex — ratio of hyperinflation area to proportion of ventilated lungs (A_{VENT}); T_{HYPER}/T_{INSP} — ratio of hyperinflation time to inspiratory time; VR — ventilatory ratio; Z_{HYPER} — ratio of hyperinflation area to ventilation area; Z_{RVD} — ratio of regional ventilation delay zone to ventilation area; CI — confidence interval; NIV —noninvasive ventilation; RR — respiratory rate.

The study found that the «Strain-vent index» (Z_{HYPER}/A_{VENT}) had good predictive value on the day of NIV initiation: 27.6 (22.0–48.6) in the success group and 55.6 (37.2–62.4) in the failure group (AUROC 0.81, $p = 0.005$, cut point 45.0, Se 65 %, Sp 78 %) and on the last day: 26.9 (16.4–37.2) in the success group and 57.9 (42 .4–68.8) in the failure group, (AUROC 0.92, $p < 0.0001$, cut-off point 39.7, Se 85 %, Sp 89 %) (Figure 1, D).

The T_{HYPER}/T_{INSP} ratio (Figure 1, E) also showed its prognostic value on the last day of NIV. The NIV success patients had a ratio of 37.5 (31.0–47.9), while NIV failure patients had a ratio of 65.3 (43.7–88.4) (AUROC 0.876, $p = 0.001$, cut-off 52.7, Se 71 %, Sp 100 %). ROC analysis demonstrated good discrimination of these values (see Table 2). A_{VENT}, Z_{RVD}, and inspiratory time did not differ significantly between patients with NIV failure and NIV success (see Table 2). The ROX index and PaO_2/FiO_2 (but not VR) also showed a good prediction of NIV failure 48 hours after the start of NIV (day 3) (Figure 1, F, see Table 2).

Discussion

The majority of ICU patients with COVID-19 belong to the category of elderly and senile people with concomitant diseases, protein-energy deficiency, and immunosuppression during therapy with glucocorticoids and interleukin-6 inhibitors, which increases the risk of developing infectious and non-infectious complications, as well as death when using invasive ventilation [12].

NIV is an effective treatment that not only reduces the number of infectious complications in patients with immunosuppression, but can also help reduce the burden on staff during a pandemic and increased load on the ICU. It can be carried out outside the ICU, providing more comfortable conditions for the patient. Several observational studies and their meta-analysis have demonstrated the high effectiveness of NIV outside the ICU [13].

Although non-invasive ventilation (NIV) has obvious advantages, its use poses several problems that require special attention. It may lead to ventilator-associated lung injury (VALI) and patient-induced lung injury (P-SILI) which can exacerbate acute respiratory distress syndrome (ARDS) in patients. However, the exact risk factors and threshold values for damaging parameters during NIV for hypoxemic acute respiratory failure (ARF) caused by COVID-19 are yet to be identified, making the assessment of VALI and P-SILI a complex and unresolved issue [14]. The effectiveness of NIV for patients with progression of respiratory failure remains low, and the threshold for tracheal intubation is uncertain, especially for patients who were already receiving low-flow oxygen or continuous positive airway pressure (CPAP) outside the intensive care unit (ICU) and were transferred to the ICU due to progression of ARF. The advantage of using NIV in the ICU in such cases is less apparent [15]. Additionally, NIV may cause a delay in tracheal intubation and increase P-SILI, which depends on various factors including ventilation parameters, interface, and respiratory system mechanics [16]. However, there is limited data on predicting NIV failure based on physiological respiratory parameters [17–19].

The EIT curve is a wave plethysmogram of changes in the impedance of the chest tissue (Z), obtained as a total pixel image for one respiratory cycle, which can also be divided into regions of interest (ROI). In our study, we divided into only two areas of interest (right and left ventral and dorsal squares). The summed change in the impedance range by square is expressed by the impedance delta variable (ΔZ). It closely correlates with changes in the airiness of the lung tissue [6]. ΔZ comprises two main components: variability of the tidal volume — ΔTV (Tidal Variation), and variability of end-expiratory lung impedance — ΔEELI (End-Expiratory Lung Impedance), which is an analogue of end-expiratory lung volume EELV (End-Expiratory Lung Volume). When PEEP changes and the airiness of the lung tissue changes, ΔEELI will also change [20].

The vast majority of studies that used EIT to select optimal ventilatory parameters for ARDS both before and during the COVID-19 pandemic have been conducted in patients undergoing invasive ventilation with neuromuscular blockade. These studies aimed to identify the ideal level of PEEP as the optimal balance between the area of zones of collapse and overinflation of lung tissue during exhalation (ΔEELI) [9, 21–23]. Bachmann M.C., Morais C., et al. (2018), published a review of the capabilities of EIT in the

ICU for patients with ARDS [9], which included a detailed analysis of the technical concepts and clinical application of EIT to improve the quality of invasive respiratory support. The authors questioned whether EIT as a continuous monitoring method could be superior to standard imaging techniques such as lung CT to help guide the selection of optimal respiratory support parameters for ARDS, since the lungs of a healthy patient and a patient with ARDS are strikingly different and great care must be taken in selecting parameters. The review also highlights the benefits of EIT for detecting pneumothorax early on during recruitment maneuvers, as well as the ability of EIT to map ventilation and perfusion and assess regional ventilation delays. In conclusion, the review presents EIT as a promising modern method for patients undergoing invasive ventilation.

Costa E.L. et al. used a stepwise decrease in the PEEP level to find the optimal PEEP level during mechanical ventilation with neuromuscular blockade as a balance between overinflation and collapse of the alveoli [24]. Philip van der Zee P., Somhorst P., et al. (2020) published a similar study in which they selected the optimal level of PEEP in patients with COVID-19-associated ARDS by assessing the decrease and increase in the impedance of the lung tissue, as well as calculating the compliance for each "step" of PEEP as:

$$\text{Compliance pixel} = \Delta Z / (P_{plat} - PEEP).$$

They also used stepwise reduction of PEEP to find a balance between hyperinflation and collapse during invasive mechanical ventilation [25]. Perier F. et al. EIT was used to map ventilation and perfusion in prone and supine patients to explain the success of prone positioning in patients with COVID-19 [26].

The RECRUIT study, which was published recently, involved 108 patients with ARDS. In this study, EIT was used to identify the potential for lung recruitment and to select a safe level of PEEP. The selection of PEEP was individualized by EIT, and it will assist in determining the appropriateness of recruitment [27].

Despite numerous studies conducted on patients undergoing mechanical ventilation, there is a limited number of studies that explore the use of EIT during spontaneous breathing. Of particular interest are studies in patients with pulmonary diseases [28]. In 2021, was published a pilot study on the use of EIT in patients during NIV with COVID-19-associated ARDS which was aimed to measure changes the level of ΔEELV (end-expiratory lung volume) at different CPAP levels. The authors did not evaluate one of the main causes of the disease progression in the lungs during NIV — overinflation of the alveoli during inspiration. The study included 10 patients with mild ARDS. ΔEELI measurements were taken when the CPAP level was decreased from 12 to 6 mbar in supine and prone positions. A decrease in ΔEELI by less than 40 % during CPAP decrease was a predictor of NIV failure. But this study did not address lung overinflation, as well as P-SILI during NIV [29].

EIT technology causes a color change in the EIT picture during inspiration, where each patient experiences a shift from black (lowest impedance, least airiness) to white (highest impedance, most airiness). It is important to note that the color is not standardized for a certain impedance value.

Thus, the white zones are the zones with the highest change in impedance from the original (or the highest local VT, or compliance). However, a change in color to white does not necessarily mean that the lung is overinflated. If this happens evenly, we can only say about a uniform increase in the airiness of the lungs during inspiration.

Therefore, there will always be a wide area number of white zone during inspiration if automatic scaling is selected. However, if the EIT picture shows regional differences in the color of the EIT picture (the simultaneous existence of white, blue, dark blue, and black) at the height of inspiration, we can assume that the white zones correspond to zones of alveolar overinflation. Taking into account the initial volume of lung tissue damage (the volume of the lesion on the CT scan was 75–100 %), we can assume the presence of overstretched alveoli (strain, volutrauma).

In 2016, a group of scientists conducted a study on healthy volunteers during spontaneous breathing of atmospheric air, aiming to evaluate the correlation of impedance changes with VT during quiet and forced breathing. Changes in impedance strongly correlated with spirometric data, both during quiet breathing and during forced breathing with maximum effort. This study can confirm our theory because the higher the impedance change, the more white pixels there will be at the inhalation height. However, the study did not evaluate the distribution of white areas and their homogeneity [30].

Since our patients had nonhomogeneous lung ventilation, which was expressed in zones with different changes in impedance during breathing (from black-blue to dark blue — poor ventilation or from black to bright white — excessive ventilation), we believe that the zones that were colored white corresponded to zones of excess ventilation compared to blue zones. However, in a healthy person with uniform ventilation, we would observe a different picture: all zones at the height of inspiration would be uniformly white because they would reach the maximum level of impedance change at the same time. Accordingly, the presence of uneven ventilation, visualized by EIT, may allow us to identify bright white zones as zones of alveolar overextension (strain).

The time of exposure to injury will influence the extent of lung injury. We assessed the time of existence of white zones as the time of existence of alveolar overdistension (strain) during NIV and confirmed the role of overinflation time for the prediction of NIV failure.

Limitations of the study

The limitations of our study were its observational nature, small sample size, and the assumptions we made to assess the "white" zones as zones of overinflation of the al-

veoli when they are simultaneously present with the "blue" ventilation zones.

We consider this work as a preliminary attempt to propose a new hypothesis regarding the feasibility of non-invasive assessment of areas of alveolar hyperinflation using EIT in patients undergoing NIV. Further research on this issue is needed.

Conclusion

EIT can predict NIV failure in moderate-to-severe COVID-19-associated ARDS based on an assessment of areas of alveolar overinflation. Further research is required to explore this theory.

Disclosure. The authors declare no competing interests.

Author contribution. All authors according to the ICMJE criteria participated in the development of the concept of the article, obtaining and analyzing factual data, writing and editing the text of the article, checking and approving the text of the article.

Ethics approval. This study was approved by the local Ethical Committee of Sechenov First Moscow State Medical University (reference number: 20-20-15.07.2020).

Funding source. This study was not supported by any external sources of funding.

Data Availability Statement. The data that support the findings of this study are available from the corresponding author upon reasonable request.

Author's ORCID:

Krasnoshchekova A.P. — 0000-0001-6986-1368
Yaroshetskiy A.I. — 0000-0002-1484-092X
Serkova T.S. — 0000-0003-1629-6240
Merzhoeva Z.M. — 0000-0002-3174-5000
Trushenko N.V. — 0000-0002-0685-4133
Nuralieva G.S. — 0000-0002-4726-4906
Tsareva N.A. — 0000-0001-9357-4924
Avdeev S.N. — 0000-0002-5999-2150

References

[1] *Roesthuis L., van den Berg M., van der Hoeven H*. Advanced respiratory monitoring in COVID-19 patients: use less PEEP! Crit Care. 2020; 24(1): 230. DOI: 10.1186/s13054-020-02953-z

[2] *Sella N., Zarantonello F., Andreatta G., et al.* Positive end-expiratory pressure titration in COVID-19 acute respiratory failure: electrical impedance tomography vs. PEEP/FiO2 tables. Crit Care. 2020; 24(1): 540. DOI: 10.1186/s13054-020-03242-5

[3] *Yaroshetskiy A.I., Avdeev S.N., Politov M.E., et al*. Potential for the lung recruitment and the risk of lung overdistension during 21 days of mechanical ventilation in patients with COVID-19 after noninvasive ventilation failure: the COVID-VENT observational trial. BMC Anesthesiol. 2022; 22(1): 59. DOI: 10.1186/s12871-022-01600-0

[4] *Грицан А.И., Авдеев Н.В., Демко И.В. и др*. Анализ результатов проведения искусственной вентиляции легких у пациентов с инфекцией COVID-19, осложненной острым респираторным дистресс-синдромом. Анестезиология и реаниматология. 2021; 6: 52–60. DOI: 10.17116/anaesthesiology202106152 [*Gritsan A.I., Avdeev N.V., Demko I.V., et al.* Results of mechanical ventilation in patients with COVID-19 complicated by acute respiratory distress syndrome. Russian Journal of Anaesthesiology and Reanimatology. 2021;(6):52–60. DOI: 10.17116/anaesthesiology202106152 (In Russ)]

[5] *Tsolaki V.S., Zakynthinos G.E, Mantzarlis K.D., et al*. Driving Pressure in COVID-19 Acute Respiratory Distress Syndrome Is Associated with Respiratory Distress Duration before Intubation. Am J Respir Crit Care Med. 2022; 204(4): 478–81. DOI: 10.1164/rccm.202101-0234LE

[6] *Victorino J.A., Borges J.B., Okamoto V.N., et al*. Imbalances in regional lung ventilation: a validation study on electrical impedance tomography. Am J Respir Crit Care Med. 2004; 169(7): 791–800. DOI: 10.1164/rccm.200301-133OC

[7] *Hentze B., Muders T., Luepschen H., et al*. Regional lung ventilation and perfusion by electrical impedance tomography compared to single-photon emission computed tomography. Physiol Meas. 2018; 39(6): 065004. DOI: 10.1088/1361-6579/aac7ae

[8] *Wrigge H., Zinserling J., Muders T., et al*. Electrical impedance tomography compared with thoracic computed tomography during a slow inflation maneuver in experimental models of lung injury. Crit Care Med. 2008; 36(3): 903–9. DOI: 10.1097/CCM.0B013E3181652EDD

[9] *Bachmann M.C., Morais C., Bugedo G., et al*. Electrical impedance tomography in acute respiratory distress syndrome. Crit Care. 2018; 22(1): 263. DOI: 10.1186/s13054-018-2195-6

[10] *Patrick W., Webster K., Ludwig L., et al*. Noninvasive positive-pressure ventilation in acute respiratory distress without prior chronic respiratory failure. Am J Respir Crit Care Med. 1996; 153(3): 1005–11. DOI: 10.1164/ajrccm.153.3.8630538

[11] Временные методические рекомендации: профилактика, диагностика и лечение новой коронавирусной инфекции (COVID-19) версия 10 (08.02.2021). Available at: https://static-0.minzdrav.gov.ru/system/attachments/attaches/000/054/588/original/Временные_МР_COVID-19_

(v.10)-08.02.2021_(1).pdf [Temporal clinical guideline on prophylaxis, diagnostics and treatment of new coronavirus disease (COVID-19), version 10 (08.02.2021). Available at: https://static-0.minzdrav.gov.ru/system/attachments/attaches/000/054/588/original/Временные_MP_COVID-19_(v.10)-08.02.2021_(1).pdf]

[12] *Chong E., Chan M., Tan H.N., et al*. COVID-19: Use of the Clinical Frailty Scale for Critical Care Decisions. J Am Geriatr Soc. 2020; 68(6): E30–E32. DOI: 10.1111/jgs.16528

[13] *Cammarota G., Esposito T., Azzolina D., et al*. Noninvasive respiratory support outside the intensive care unit for acute respiratory failure related to coronavirus-19 disease: a systematic review and meta-analysis. Crit Care. 2021; 25(1): 268. DOI: 10.1186/s13054-021-03697-0

[14] *Grieco D.L., Menga L.S., Eleuteri D., et al*. Patient self-inflicted lung injury: implications for acute hypoxemic respiratory failure and ARDS patients on non-invasive support. Minerva Anestesiol. 2019; 85(9): 1014–23. DOI: 10.23736/S0375-9393.19.13418-9

[15] *Wendel-Garcia P.D., Mas A., González-Isern C., et al*; UCIsCAT study group. Non-invasive oxygenation support in acutely hypoxemic COVID-19 patients admitted to the ICU: a multicenter observational retrospective study. Crit Care. 2022; 26(1): 37. DOI: 10.1186/s13054-022-03905-5

[16] *Weaver L., Das A., Saffaran S., et al*. High risk of patient self-inflicted lung injury in COVID-19 with frequently encountered spontaneous breathing patterns: a computational modelling study. Ann Intensive Care. 2021; 11(1): 109. DOI: 10.1186/s13613-021-00904-7

[17] *Tonelli R., Fantini R., Tabbì L., et al*. Early Inspiratory Effort Assessment by Esophageal Manometry Predicts Noninvasive Ventilation Outcome in De Novo Respiratory Failure. A Pilot Study. Am J Respir Crit Care Med. 2020; 202(4): 558–67. DOI: 10.1164/rccm.201912-2512OC

[18] *Esnault P., Cardinale M., Hraiech S., et al*. High Respiratory Drive and Excessive Respiratory Efforts Predict Relapse of Respiratory Failure in Critically Ill Patients with COVID-19. Am J Respir Crit Care Med. 2020; 202(8): 1173–8. DOI: 10.1164/rccm.202005-1582LE

[19] *Dargent A., Hombreux A., Roccia H., et al*. Feasibility of non-invasive respiratory drive and breathing pattern evaluation using CPAP in COVID-19 patients. J Crit Care. 2022; 69: 154020. DOI: 10.1016/j.jcrc.2022.154020

[20] *Hinz J., Hahn G., Neumann P., et al*. End-expiratory lung impedance change enables bedside monitoring of end-expiratory lung volume change. Intensive Care Med. 2003; 29(1): 37–43. DOI: 10.1007/s00134-002-1555-4

[21] *Zhao Z., Lee L.C., Chang M.Y., et al*. The incidence and interpretation of large differences in EIT-based measures for PEEP titration in ARDS patients. J Clin Monit Comput. 2020; 34(5): 1005–13. DOI: 10.1007/s10877-019-00396-8

[22] *Sun X.M., Chen G.Q., Wang Y.M., et al*. Derecruitment volume assessment derived from pressure-impedance curves with electrical impedance tomography in experimental acute lung injury. J Int Med Res. 2020; 48(8): 300060520949037. DOI: 10.1177/0300060520949037

[23] *Perier F., Tuffet S., Maraffi T., et al*. Electrical impedance tomography to titrate positive end-expiratory pressure in COVID-19 acute respiratory distress syndrome. Crit Care. 2020; 24(1): 678. DOI: 10.1186/s13054-020-03414-3

[24] *Costa E.L., Borges J.B., Melo A., et al*. Bedside estimation of recruitable alveolar collapse and hyperdistension by electrical impedance tomography. Intensive Care Med. 2009; 35(6): 1132–7. DOI: 10.1007/s00134-009-1447-y

[25] *van der Zee P., Somhorst P., Endeman H., et al*. Electrical Impedance Tomography for Positive End-Expiratory Pressure Titration in COVID-19-related Acute Respiratory Distress Syndrome. Am J Respir Crit Care Med. 2020; 202(2): 280–4. DOI: 10.1164/rccm.202003-0816LE

[26] *Perier F., Tuffet S., Maraffi T., et al*. Effect of Positive End-Expiratory Pressure and Proning on Ventilation and Perfusion in COVID-19 Acute Respiratory Distress Syndrome. Am J Respir Crit Care Med. 2020; 202(12): 1713–7. DOI: 10.1164/rccm.202008-3058LE

[27] *Jonkman A.H., Alcala G.C., Pavlovsky B., et al*; Pleural Pressure Working Group (PLUG). Lung Recruitment Assessed by Electrical Impedance Tomography (RECRUIT): A Multicenter Study of COVID-19 Acute Respiratory Distress Syndrome. Am J Respir Crit Care Med. 2023; 208(1): 25–38. DOI: 10.1164/rccm.202212-2300OC

[28] *Krueger-Ziolek S., Schullcke B., Gong B., et al*. EIT based pulsatile impedance monitoring during spontaneous breathing in cystic fibrosis. Physiol Meas. 2017; 38(6): 1214–25. DOI: 10.1088/1361-6579/aa69d5

[29] *Rauseo M., Mirabella L., Laforgia D., et al*. A Pilot Study on Electrical Impedance Tomography During CPAP Trial in Patients With Severe Acute Respiratory Syndrome Coronavirus 2 Pneumonia: The Bright Side of Non-invasive Ventilation. Front Physiol. 2021; 12: 728243. DOI: 10.3389/fphys.2021.728243

[30] *Ngo C., Leonhardt S., Zhang T., et al*. Linearity of electrical impedance tomography during maximum effort breathing and forced expiration maneuvers. Physiol Meas. 2017; 38(1): 77–86. DOI: 10.1088/1361-6579/38/1/77